APPLIED ORGANOMETALLIC CHEMISTRY, VOL. 9, 667–673 (1995)

Chemical Vapour Deposition of Germanium-containing Films by IR Laser-induced Decomposition of Ethoxy(trimethyl)germane

Radek Fajgar,* Zdeněk Bastl,† Jaroslav Tláskal‡ and Josef Pola*§
Academy of Sciences of the Czech Republic, * Institute of Chemical Process Fundamentals, 165 02 Prague 6–Suchdol, Rozvojova 135, † J. Heyrovský Institute of Physical Chemistry, 182 23 Prague 8, and ‡ Institute of Inorganic Chemistry, 25 068 Řež, near Prague, Czech Republic

Carbon Dioxide (CO_2) laser-induced decomposition of ethoxy(trimethyl)germane (ETG) results in a substantial stripping of organic substituents from germanium and leads to deposition of organogermanium films, the composition of which is dependent on the mode of laser irradiation. Direct absorption of laser radiation in ETG affords material rich in Germanium, while a sulfur hexafluoride (SF_6)-photosensitized process produces a deposit composed of Germanium, Carbon, Hydrogen and Oxygen. The deposited materials can be modified by chemical reactions with acetic anhydride and atmospheric moisture.

Keywords: chemical vapour deposition; laser-induced decomposition; organogermanium film; ethoxy(trimethyl)germane

INTRODUCTION

The preparation of polymeric organogermanium oxides, analogous to silicones, has long been of interest in organogermanium chemistry, but traditional methods of preparing these organogermanium polymers using hydrolysis of dihalogermanes,[1-3] dialkoxygermanes,[4-6] organogermanium trichlorides[6-9] or tetraalkoxygermanes[10] have been recognized to yield only low-molecular-weight, water-soluble oligomers, germanium dioxide or digermoxanes. An alternative approach to the production of polymeric organo-oxogermanes is the radical decomposition of alkyl(alkoxy)germanes in the gas phase. Previous studies on metallo-organic chemical vapour deposition (MOCVD) reveal that pyrolytic[11] and plasma-induced[12] decomposition of tetraethoxygermane affords only germanium dioxide, but laser-induced decomposition of tetramethoxygermane yields films of reactive organo-oxogermanium polymers.[13]

These different results[11-13] reflect the commonly shared view that the nature of deposited materials is affected by the structure of the gaseous precursor and by the conditions of precursor decomposition; this has been well documented even for laser-induced MOCVD using organogermanes.[13-18]

In a continuation of our previous studies on IR laser-induced MOCVD of polyorgano-oxogermanes from tetramethoxygermane[13] and of germanium from tetramethylgermane,[17] we report in this paper the gas-phase carbon dioxide (CO_2) laser-induced decomposition of ethoxy(trimethyl)germane (ETG) and assess the use of direct infrared multiphoton decomposition (IRMPD) as well as sulphur hexafluoride (SF_6) photosensitized decomposition (PSD) of ETG as a technique for preparation (deposition) of polymeric organo-oxogermanes.

EXPERIMENTAL

Laser irradiation experiments were performed on gaseous samples of ETG and ETG–SF_6 compounds contained in a cylindrical glass reactor (10 cm × 3.6 cm i.d.), equipped with sodium chloride (NaCl) windows, a PTFE stopcock and a sleeve with rubber septum. A grating-tuned transversely excited atmospheric (TEA) CO_2 laser[19] was operated at a repetition frequency of 1 Hz (energy in pulse 0.28 J cm^{-2}) on the R(12) line of the 00°1–02°0 transition (1073.2 cm^{-1}) to achieve absorption in ETG. A grating-tuned continuous-

---

§ Author to whom correspondence should be addressed.

CCC 0268–2605/95/080667–07
© 1995 by John Wiley & Sons, Ltd.

Received 21 September 1994
Accepted 27 February 1995

wave CO_2 laser[20] (output 10 W) operating on the P(20) line of the 00°1–02°0 transition (944.2 cm^{-1}) was chosen for the irradiation of the ETG–SF_6 mixture when absorption in SF_6 was effective. The laser beam of the pulsed and continuous radiation was focused at the centre of the horizontally positioned reactor using a Ge or NaCl lens, and the substrate (NaCl, potassium bromide (KBr) glass or aluminium) for the deposit was housed 1.5 cm beneath the focal point. The laser beam energy was measured with a laser energy pyroceramic sensor (Charles University, ml-1JU model) or a Coherent Model 201 power meter, and the laser line used for the irradiation was verified with a model 16-A spectrum analyser (Optical Engineering Co.).

The samples for laser irradiation were prepared by a standard vacuum-line technique and the pressure of ETG was measured by a Barocel pressure transducer (model 1570). The IR spectra before and after irradiation were recorded with a Specord 75 model (Zeiss) IR spectrometer. The depletion of ETG was monitored at 810 and 1040 cm^{-1}. Gaseous products of the laser-induced decomposition of ETG were identified by their absorption spectra (methane 1300 cm^{-1}, ethene 950 cm^{-1}, ethyne 730 cm^{-1} and acetaldehyde 1746 cm^{-1}), by their mass fragmentation and by their retention times. For the latter purpose, helium was expanded into the reactor to atmospheric pressure and gaseous samples were injected into a GC/MS (Shimadzu QP 1000) quadrupole mass spectrometer (column 1.2 m long packed with Porapak P, programmed temperature 25–160 °C). The amounts of gaseous compounds were determined by using the absorptivity of the diagnostic (strong, non-overlapping) bands and the comparison with molar absorptivities measured with authentic samples (cm^{-1}, $10^3 \times kPa^{-1} cm^{-1}$): ETG, 1040, 64 and 810, 65; CH_4, 1300, 30; C_2H_2, 730, 94: C_2H_4, 950, 70; CH_3CHO, 1746, 58.

The deposit on glass or NaCl substrates was investigated by means of X-ray photoelectron spectroscopy, scanning electron microscopy, UV/Vis and IR spectroscopy.

ESCA measurements were made using a VG ESCA 3 MkII electron spectrometer. The pressure of residual gases during accumulation of the spectra was in the 10^{-6} Pa range. The measurements were performed using AlK_α (1486.6 eV) radiation. The spectrometer was operated in the fixed-analyser transmission mode with a pass energy of 20 eV giving a resolution of 1.1 eV on the Au $f_{7/2}$ line. The preparation chamber of the spectrometer was equipped with a cold cathode ion gun.

The spectra of Ge 2*p*, 3*d*, C 1*s* and O 1*s* photoelectrons and Ge $L_3M_{45}M_{45}$ Auger electrons were measured. The ratios of atomic concentrations were determined by correcting the photoelectron peak areas for their cross-sections[21] and by taking into account the dependence of the photoelectron mean free path and analyser transmission on electronic kinetic energy.[22, 23] The overlapping spectral features were resolved into individual components of Gaussian–Lorentzian shape using a modified version of the damped non-linear squares procedure published by Hughes and Sexton.[24] For binding energy data we estimated the error limit of ±0.2 eV. The estimated accuracy of the calculated ratios of atomic concentrations amounted to ±10%.

UV/Vis absorption spectra of the deposit were measured, using a Hewlett-Packard 8451A spectrometer, in the range 120–900 nm.

Scanning electron microscopy (SEM) studies of the deposit were performed on an ultra-high vacuum Tesla BS 350 instrument equipped with an energy-dispersive analyser of X-ray radiation, Edax 9100/65. An ECON detector in the shield mode (plastic window) was used for qualitative determination of light elements. The morphology of the samples was investigated mostly using an accelerating voltage of 4 kV.

ETG samples as well as authentic samples of trimethylgermane and tetramethylgermane were prepared as reported[10] and distilled under vacuum before use. Sulphur hexafluoride was a commercial sample from Fluka.

RESULTS AND DISCUSSION

Infrared multiphoton decomposition (IRMPD)

Focused irradiation by the CO_2 laser (0.28 J in pulse) in the strong absorption band (ν_{Ge-O} mode) of ETG at 1073 cm^{-1} results (Figs 1 and 2) in the depletion of ETG and formation of methane, ethene, ethyne, acetaldehyde, carbon monoxide and a compound whose structure was tentatively assigned to $(H_2CH_3Ge)_2O$ [infrared absorption at 2035 cm^{-1}; mass spectrum – $CH_4(CH_3)_2Ge_2O^+$ (characteristic mass range 190–202)]. A significant amount of a solid brown material, deposited

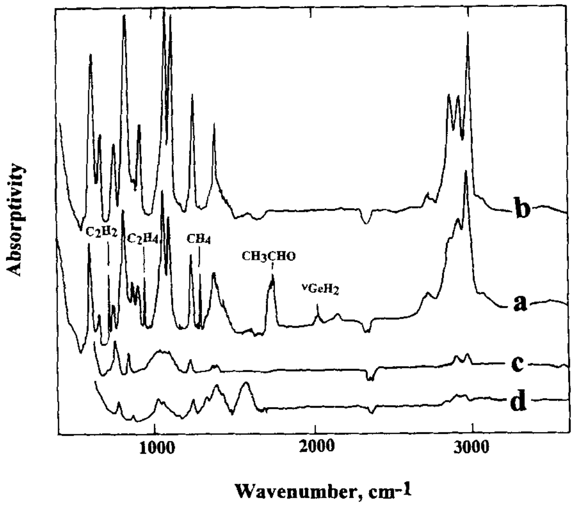

Figure 1 IR spectra of the irradiated [900 pulses, (**a**)] and initial (**b**) ETG, and of the solid deposit (**c**) and the deposit treated with acetic anhydride (**d**).

all over the inside of the reactor, is produced concomitantly. Mass balance measurement (IR spectral determination of amounts of gaseous products) (Fig. 3) is consistent with approximately 80% of carbon being used for the formation of the gaseous products. A very weak absorption band at 2035 cm^{-1} and the high molar absorptivity of organogermanium hydrides at this wavelength[14] lead us to believe that the volatile digermoxane is formed only at pressures lower than 0.01 kPa, which implies that almost all the germanium, less than 20% of the carbon and less than 60% of the oxygen from the ETG is incorporated in the deposited material. This estimation is consistent with the stoichiometry of the deposit as determined by X-ray photoelectron spectroscopy (XPS) analysis (Table 1).

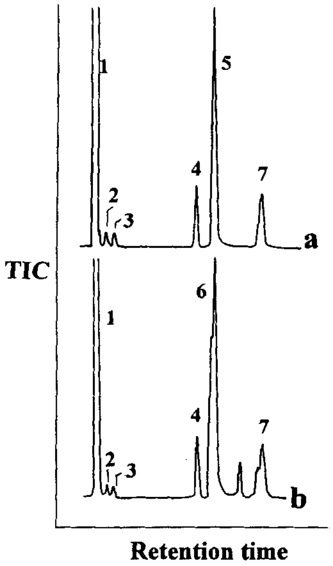

Figure 2 Typical GC–MS trace of the irradiated ETG (**a**) and ETG–SF_6 (**b**). Peak identification: 1, air; CO; 2, CH_4; 3, C_2H_4, C_2H_2; 4, CH_3CHO; 5, ETG, C_2H_5OH; 6, $(CH_3)_4Ge$, $(CH_3)_3GeH$, ETG, C_2H_5OH; 7, $(CH_3H_2Ge)_2O$.

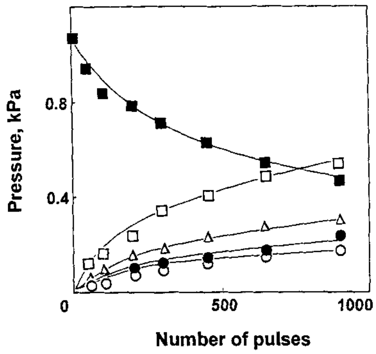

Figure 3 Distribution of volatile products in IRMPD of ETG: ■, ETG; △, C_2H_4; ●, C_2H_2; ○, CH_3CHO; □, CH_4).

Photosensitized decomposition (PSD)

Focused irradiation by the continuous-wave (cw) CO_2 laser on ETG–SF_6 (each component 0.7 kPa) mixtures (incident energy 40 W cm^{-2}) tuned to

Table 1 XPS core level binding energies, Auger parameters (eV) and composition of the deposits.

Source of deposit	Ge $2p_{3/2}$	Ge $3d$	Auger parameter[a]	Stoichiometry
IRMPD	1219.3	30.3	1174.3	$Ge_{1.0}C_{1.1}O_{1.1}$
IRMPD[b]	1217.9	29.9	1174.7	$Ge_{1.0}C_{0.3}O_{0.1}$
PSD	1220.3	32.4	1171.4	$Ge_{1.0}C_{4.8}O_{1.8}$
PSD[b]	1218.1	30.1	1174.5	$Ge_{1.0}C_{1.8}O_{0.8}$
IRMPD/Ac_2O	1218.2	29.9	—[c]	$Ge_{1.0}C_{0.9}O_{1.0}$
	1220.3	32.3		
IRMPD/Ac_2O[d]	1217.3	—	—[c]	$Ge_{1.0}C_{0.4}O_{1.0}$
	1219.3	—		
	1221.0	—		
—	1217.2	29.6	1174.7	Clean Ge[e]
	1220.4	33.3	1170.9	GeO_2[e]

[a] Value of Auger parameter based on Ge $3d$ peak.

[b] After 10 min of sputtering with argon ions (energy 5 keV, ion current approx. 40 μA).

[c] Because of overlap of Auger peaks which could not be separated, the Auger parameter values were not calculated.

[d] After 1 min of sputtering with argon ions (energy 3.5 keV, ion current 40 μA).

[e] Reference (commercial) samples of polycrystalline germanium and GeO_2 respectively.

the strong absorption band of SF_6 at 944 cm^{-1} has a similar effect to direct absorption of the laser radiation in ETG. SF_6 acts as an energy-conveying agent[25,26] and induces homogeneous decomposition of ETG. Irradiation times shorter than 40 s were sufficient to achieve approximately 60% decomposition. Gaseous products formed included those observed upon IRMPD of ETG and also tetramethylgermane and trimethylgermane (Fig. 2b). Formation of a brown powder-like material was observed as well, but its amount was smaller than in IRMPD.

The similarity of the main volatile products in IRMPD and particle-size determination (PSD) of ETG indicates that the major steps contributing to the decomposition are the same. The analysis of the deposited materials by XPS (Table 1), as well as the amounts of gaseous products (Fig. 3) are in line with a substantial cleavage of organic moieties from germanium. The cleavage of the Ge–O and Ge–C bonds is easier than that of the O–C bond (homolytic bond dissociation energy 300 kJ mol^{-1},[27] 240 kJ mol^{-1},[10] and 340 kJ mol^{-1}, respectively). The initial Ge–C and Ge–O cleavages in ETG are obviously followed by radical reactions with parent ETG as hydrogen abstraction from the OCH_2CH_3 (major, Eqn [2]) or OCH_2CH_3 (minor, Eqn [3]) units, loss of acetaldehyde (major, Eqn [4]), or ethene (minor Eqn [5]). These products can also be formed by direct four-centre β-elimination reactions (Eqns [6], [7]). Second-order radical reactions, e.g. disproportionation of an ethoxy radical,[29,30] is less likely. Decomposition of acetaldehyde[31] (Eqn [8]) and ethanol[32] (Eqn [9]) can occur, too. The proposed steps are given in Eqns [1]–[9].

$$\cdot\overset{|}{\underset{|}{\mathrm{Ge}}}\text{—}OCH_2CH_3 + CH_3^{\cdot} \leftarrow ETG \rightarrow CH_3\text{—}\overset{|}{\underset{|}{\mathrm{Ge}}}{}^{\cdot} + {}^{\cdot}OCH_2CH_3 \quad [1]$$

$$CH_3^{\cdot} + (CH_3)_3GeOCH_2CH_3 \rightarrow CH_4 + (CH_3)_3GeOCH^{\cdot}CH_3 \quad [2]$$

$$CH_3^{\cdot} + (CH_3)_3GeOCH_2CH_3 \rightarrow CH_4 + (CH_3)_3GeOCH_2CH_2^{\cdot} \quad [3]$$

$$(CH_3)_3GeOCH^{\cdot}CH_3 \rightarrow (CH_3)_3Ge^{\cdot} + CH_3CHO \quad [4]$$

$$(CH_3)_3GeOCH_2CH_2^{\cdot} \rightarrow (CH_3)_3GeO^{\cdot} + C_2H_4 \quad [5]$$

$$(CH_3)_3GeOCH_2CH_3 \rightarrow (CH_3)_3GeH + CH_3CHO \quad [6]$$

$$(CH_3)_3GeOCH_2CH_3 \rightarrow (CH_3)GeOH + C_2H_4 \quad [7]$$

$$CH_3CHO \rightarrow CH_4 + CO \quad [8]$$

$$CH_3CH_2OH \rightarrow C_2H_4 + H_2O \quad [9]$$

Formation of trimethylgermane might also occur via molecular expulsion of ethene oxide which rearranges[32,33] into acetaldehyde Eqn [10]), rather than by an unlikely[34–36] hydrogen abstraction by the $(CH_3)_3Ge^{\cdot}$ radical.

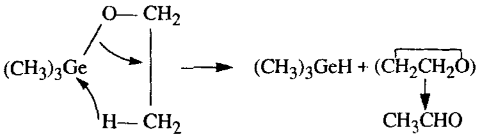

[10]

Properties of the deposit

ESCA, FTIR and SEM analyses of the deposits afforded by IRMPD and PSD of ETG reveal that the materials contain germanium, carbon, hydrogen and oxygen and that they have different properties depending on the way they were produced. Energy dispersive X-ray spectrometry (EDX)-SEM analysis of the bulk material (of ca 0.3 μm thickness) is in line with greater amounts of the deposited agglomerates and with a higher proportion of germanium in the deposit from IRMPD compared with that from PSD (Fig. 4). These results conform with the stoichiometry of superficial (up to 5 nm) layers analysed by ESCA (Table 1). The deposit from PSD contains neither fluorine nor sulphur, which shows no chemical involvement of the sensitizer. The analysis of the layers beneath those removed by ion sputtering reveals that the material deposited by IRMPD is very similar to elemental germanium, while that obtained by PSD contains, apart from germanium, carbon and oxygen also. The amounts of oxygen in superficial layers of both deposits is higher than it would be if it corresponded to the observed Ge–O cleavage/formation of acetaldehyde and ethanol, indicating that superficial layers incorporate oxygen from the atmosphere. The Auger parameters for the unchanged and ion-sputtered deposits show that the IRMPD-originated material contains elemental germanium, while that obtained from PSD incor-

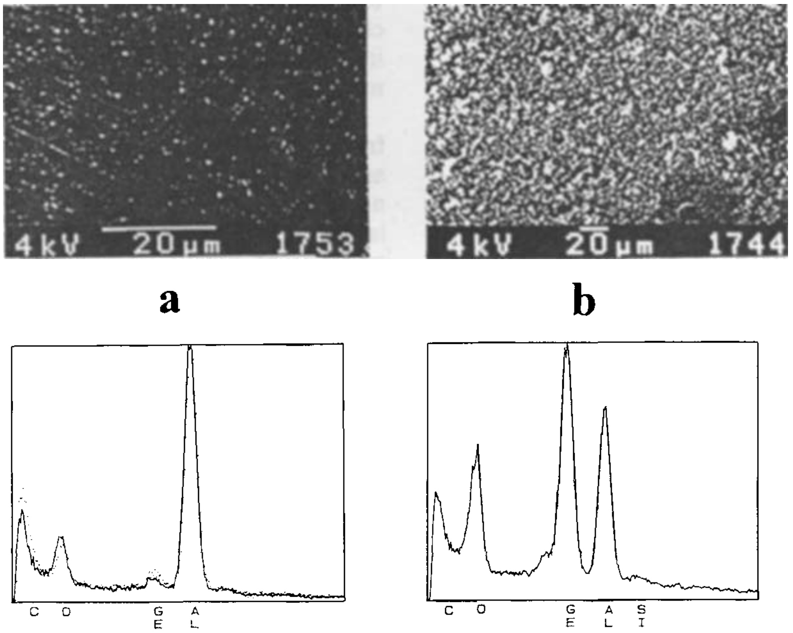

Figure 4 SEM image and EDX-SEM trace of the deposit afforded by PSD (**a**) and IRMPD (**b**).

porates superficial GeO_2, elemental germanium being incorporated only in deeper layers.

Optical absorption data of the film obtained by IRMPD (Fig. 5) show that the absorption edge (transparency) is not reached at wavelengths lower than 800 nm.

The deposits do not possess good adhesion to glass, sodium chloride or aluminium. They are soluble in acetone and tetrahydrofuran to form brown solutions, but are insoluble in ethanol and alkanes.

The deposits obtained from IRMPD and PSD exert a similar pattern of infrared absorption bands (770, 850, 1230, 1370–1400, 2900 and 2970 cm^{-1}; Fig. 1c); this is consistent[37, 38] with the occurrence of Ge—O—C and C—H bonds. In order to prove that the deposits contain $Ge—OC_2H_5$ groups, we examined the reactivity of the layers with water vapour and acetic anhydride. It is known that water reacts[10] with alkoxygermanes to yield GeO_2 and ethanol, and that acetic anhydride reacts (R. Fajgar, unpublished results) with ETG giving ethyl acetate and acetoxy(trimethyl)germane. We found that the introduction of air into the evacuated reactor containing a deposit from IRMPD leads to formation of ethanol (new bands at 1055, 1230 and 1400 cm^{-1} and a broad band centred at 3400 cm^{-1}), and that treatment of the same deposit with acetic anhydride vapour (exposure to acetic anhydride, evacuation and exposure to air) alters the infrared spectrum of the deposit due to the occurrence of a stronger band at 1400 cm^{-1} and a new band at 1600 cm^{-1} (Fig. 1d) which can

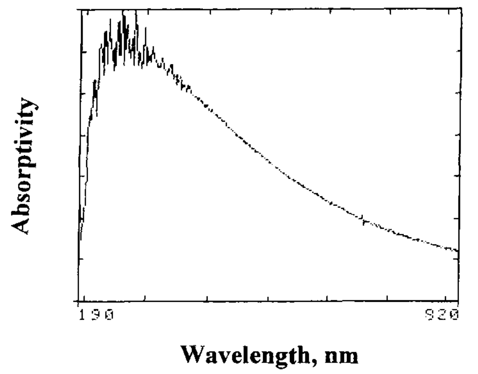

Figure 5 Absorption spectrum of the deposit from IRMPD.

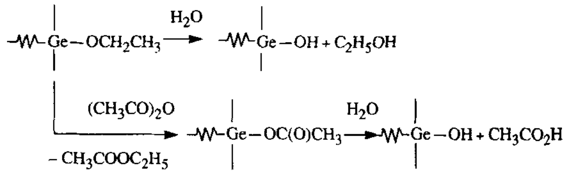

$$\text{-Ge-OCH}_2\text{CH}_3 \xrightarrow{H_2O} \text{-Ge-OH} + C_2H_5OH$$

$$\xrightarrow[-CH_3COOC_2H_5]{(CH_3CO)_2O} \text{-Ge-OC(O)CH}_3 \xrightarrow{H_2O} \text{-Ge-OH} + CH_3CO_2H$$

Scheme 1

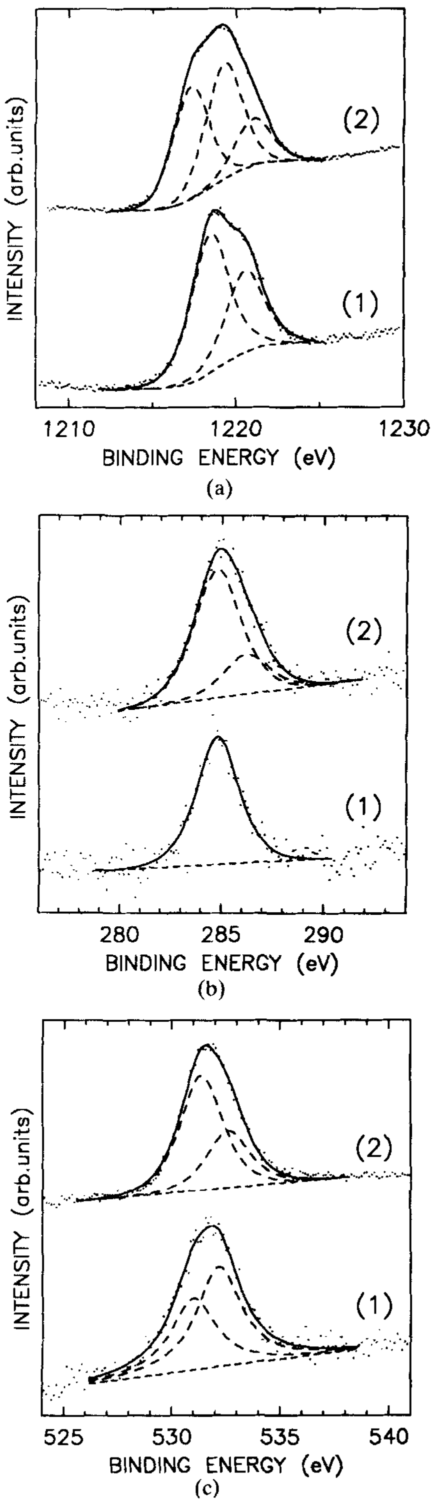

Figure 6 Spectra of Ge $2p_{3/2}$ (a), C 1*s* (b), and O 1*s* (c) photoelectrons of the deposit treated with acetic anhydride before (1) and after (2) argon ion sputtering.

be assigned to adsorbed acetic acid. These changes appear to be due to the reactions shown in Scheme 1 and they reveal that the deposited materials can be chemically modified.

The incorporation of oxygen into the deposit from IRMPD has also been confirmed by XPS analysis (Table 1); the equal amounts of germanium and oxygen in both superficial and deeper layers of the treated deposit show that the incorporation of oxygen can be enhanced by chemical treatment, and that the materials perhaps have a porous structure facilitating the penetration of reactive vapours. The approximately ten-fold increase in the oxygen content in deeper layers of the deposit from IRMPD experiments upon treatment with acetic anhydride indicates that the incorporation of oxygen cannot be solely due to reactions of Ge—OC_2H_5 groups, and that it is perhaps caused by reactions of reactive (naked) germanium centres. The nature of these reactions as well as that of the centers are at present unknown. The shape of the germanium core level spectra measured after sample treatment with acetic anhydride suggests they are composed of two peaks (Fig. 6a; Table 1) corresponding to the order of increasing binding energy likely to be ascribed to Ge—C and Ge—O and/or Ge—OH bonds, respectively. After ion sputtering, the additional peak corresponding to elemental germanium appears in the Ge $2p_{3/2}$ photoelectron spectrum. This assignment is consistent with C 1*s* and O 1*s* spectra (Fig. 6b and c, respectively).

Acknowledgement The authors thank the Grant Agency of the Academy of Sciences of the Czech Republic for financial support (grant no. 47266).

REFERENCES

1. E. G. Rochow, in Comprehensive Inorganic Chemistry, Vol. 2, J. C. Bailar, H. J. Emeléus, R. Nyholm, A. F. Trotman-Dickenson, eds. Pergamon Press, Oxford, 1973, pp. 1–41.
2. M. P. Brown and E. G. Rochow, *J. Am. Chem. Soc.* **82**, 4166 (1960).
3. W. Metlesies and H. Zeiss, *J. Am. Chem. Soc.* **82**, 3324 (1960).
4. F. Rijkens, *Organogermanium Compounds*, Germanium Research Committee, Utrecht, 1960.
5. R. Schwarz and K. G. Knauff, *Z. Anorg. Allg. Chem.* **275**, 193 (1954).
6. L. Ross and M. Drager, *Z. Naturforsch., Teil B* **39**, 868 (1984).

7. K. Haberle and M. Drager, *Z. Naturforsch., Teil B* **39**, 1541 (1984).
8. H. Puff, K. Braun, S. Franken, T. R. Kok and W. Schuh, *J. Organomet. Chem.* **349**, 293 (1988).
9. H. Puff, K. Braun, S. Franken, T. R. Kok and W. Schuh, *J. Organomet. Chem.* **335**, 167 (1987).
10. M. Lesbre, P. Mazerolles and J. Satge, *The Organic Compounds of Germanium*, Wiley, London (1971).
11. V. G. Minkina, *Izv. Akad. Nauk SSSR, Neorg. Mater.* **24**, 803 (1988), *Chem. Abstr.* **109**, 46855e.
12. M. Ya Ivanov, T. N. Kupryashkina, G. Aloyan, N. A. Ovsyannikov, E. A. Ryabenko and A. Efremov, *Sint. Soed. Plasma Soderzh. Uglevodorody*, 141 (1985); *Chem. Abstr.* **97**, 118354z.
13. J. Pola, R. Fajgar, Z. Bastl and L. Diaz, *J. Mater. Chem.* **2**, 961 (1992).
14. J. Pola, J. P. Parsons and R. Taylor, *J. Chem. Soc., Faraday Trans.* **88**, 1637 (1992).
15. J. Pola and R. Taylor, *J. Organomet. Chem.* **437**, 271 (1992).
16. J. Pola, J. P. Parsons and R. Taylor, *J. Mater. Chem.* **2**, 1289 (1992).
17. M. Jakoubková, Z. Bastl, P. Fiedler and J. Pola, *Infrared Phys. Technol.* **35**, 633 (1994).
18. A. E. Stanley, R. A. Johnson, J. B. Turner and A. H. Roberts, *Appl. Spectrosc.* **40**, 374 (1986).
19. J. Pola and S. Simeonov, *J. Chem. Soc., Perkin Trans. 2*, 101 (1991).
20. J. Pola, M. Farkačová, P. Kubát and A. Trka, *J. Chem. Soc., Faraday Trans. 1* **80**, 1499 (1984).
21. J. H. Scofield, *J. Electron Spectrosc. Relat. Phenom.* **8**, 129 (1976).
22. M. P. Seah and W. A. Dench, *Surface Interface Anal.* **1**, 1 (1979).
23. L. T. Weng, G. Vereecke, M. J. Genet, P. Bertrand and W. E. E. Stone, *Surface Interface Anal.* **20**, 179 (1992).
24. A. E. Hughes and B. A. Sexton, *J. Electron Spectrosc. Relat. Phenom.* **46**, 31 (1988).
25. W. M. Shaub and S. H. Bauer, *Int. J. Chem. Kinet.* **7**, 509 (1975).
26. D. K. Russell, *Chem. Soc. Rev.* **19**, 407 (1990).
27. Yu. Kh. Shaulov, A. K. Fedorov, G. Ya. Zueva, G. V. Borisyuk and V. G. Gendel, *Zh. Fiz. Khim.* **99**, 2081 (1970).
28. S. W. Benson, *Thermochemical Kinetics*, Wiley, New York, 1976.
29. P. Gray, R. Shaw and J. C. Thynne, *Prog. React. Kinet.* **4**, 90 (1967).
30. M. J. Gibian and R. C. Corley, *Chem. Rev.* **73**, 441 (1973).
31. T. Berces in *Comprehensive Chemical Kinetics*, Bamford, C. H. and Tipper, C. F. H. (eds), Vol. 5, Elsevier, Amsterdam, 1972.
32. W. H. Richardson and H. E. O'Neal, in *Comprehensive Chemical Kinetics*, C. H. Bamford and C. F. H. Tipper (eds), Vol. 5, Elsevier, Amsterdam, 1972.
33. M. L. Neufeld and A. T. Blades, *Can. J. Chem.* **41**, 2956 (1963).
34. J. Lucztyk, B. Maillard, S. Deycard, D. A. Lindsay and K. U. Ingold, *J. Am. Chem. Soc.* **105**, 3578 (1983).
35. J. W. Wilt, J. Lusztyk, M. Peeran and K. U. Ingold, *J. Am. Chem. Soc.* **110**, 281 (1988).
36. D. C. Carson, K. U. Ingold and L. C. Bray, *Int. J. Chem. Kinet.* **1**, 315 (1969).
37. F. Glockling, *The Chemistry of Germanium*, Academic Press, London, 1969.
38. V. C. Farmer and J. D. Russel, *Spectrochim. Acta* **18**, 461 (1962).